Development 121, 2767-2777 (1995)
Printed in Great Britain © The Company of Biologists Limited 1995

four-jointed is required for intermediate growth in the proximal-distal axis in *Drosophila*

J. Lee Villano and Flora N. Katz*

Department of Biochemistry, University of Texas Southwestern Medical Center, 5323 Harry Hines Blvd, Dallas, TX 75235-9038, USA

*Author for correspondence

SUMMARY

Genes capable of translating positional information into regulated growth lie at the heart of morphogenesis, yet few genes with this function have been identified. Mutants in the *Drosophila four-jointed* (*fj*) gene show reduced growth and altered differentiation only within restricted sectors of the proximal-distal (PD) axis in the leg and wing, thus *fj* is a candidate for a gene with this coordination function. Consistent with a position-sensitive role, we show that *fj* is expressed in a regional pattern in the developing leg, wing, eye and optic lobe. The *fj* gene encodes a novel type II membrane glycoprotein. When the cDNA is translated in an in vitro translation system in the presence of exogenous microsomal membranes, the intralumenal portion of some of the molecules is cleaved, yielding a secreted C-terminal fragment. We propose that *fj* encodes a secreted signal that functions as a positive regulator of regional growth and differentiation along the PD axis of the imaginal discs.

Key words: *four-jointed*, *Drosophila*, proximal-distal axis, imaginal disc morphogenesis

INTRODUCTION

The adult form is built upon information laid down in three axes during development: the anterior-posterior (AP), dorsal-ventral (DV) and proximal-distal (PD) axes. In the fruit fly, *Drosophila melanogaster*, a large body of work has led to a detailed description of how the AP and DV axes of the embryo are established through cascades of gene interactions very early in development (for recent reviews see: Chasan and Anderson, 1993; Driever, 1993; St. Johnston, 1993; and Sprenger and Nusslein-Volhard, 1993). As the larva is transformed into a fly, the developing adult appendages (legs, wings, antennae and halteres) use parameters arrayed in the PD axis to set distance along their length, allowing the differentiation of limb segments with different forms and functions. While genes required to initiate this axis are beginning to be identified and studied for the various imaginal discs (Campbell et al., 1993; Couso et al., 1993; Tabata and Kornberg, 1994), very little is known about how the individual limb segments read this axis in order to segregate from each other and to acquire their distinct identities. However, as the developing limbs arise from cellular epithelial sheets, the imaginal discs, it can be inferred that differentiation signals must be transferred across cell membranes via cell surface molecules and signal transduction pathways. Moreover, the different sizes and forms of the limb segments imply that some of these signals are translated into regional programs of growth (and perhaps cell death).

The imaginal discs originate as invaginations of the embryonic epidermis and are initially composed of a monolayer columnar epithelium (the disc proper) covered by a second epithelial layer, the peripodial membrane, which is later partially or completely destroyed. In those discs that give rise to adult appendages, the flat epithelium acquires a number of concentric folds as the disc cells proliferate during the larval instars. The center of these circles marks the center of the PD axis and the future distal tip of the appendage. At the onset of pupation these concentric folds evert and the limb telescopes out of the two-dimensional epithelium (reviewed in Cohen, 1993; Fristrom and Fristrom, 1993).

The functions of various genes involved in the morphogenesis of the appendages are anticipated by their expression patterns in the imaginal discs. Genes involved in initiating the PD axis are expressed in wedge-shaped patterns in the leg disc that cut across all future segment boundaries. The intersection of three of these patterns in the leg disc, representing the genes for *wingless*, *hedgehog (hh)* and *decapentaplegia*, organizes the PD axis and determines its center or origin (Campbell et al., 1993; Basler and Struhl, 1994; and Diaz-Benjumea et al., 1994). Loss of function for these genes results in loss of the entire leg, and ectopic expression can lead to abnormal initiation of ectopic legs. By contrast, genes specifying the identities and forms of individual segments along this axis might be expected to be expressed in circular patterns surrounding the center of the PD axis, in either repeating concentric rings or in blocks encompassing subsets of the prospective segments, a partial prediction of the polar coordinate model (Bryant, 1993). Genes with such expression patterns have been recovered and loss of function for some of these genes results in the loss of distal portions of the leg (*rotund*,

Kerridge and Thomas-Cavallin, 1988; Agnel et al., 1992; *Distal-less*, Cohen et al., 1989; *aristaless*, Campbell et al., 1993; Schneitz et al., 1993) or alterations in segment identity (*bric a brac*, Godt et al., 1993).

Very few genes are known whose phenotypes suggest that they are required for interpreting and elaborating intermediate values along the PD axis once it is established. One such gene is *dachshund*, in which the femur, tibia and proximal tarsal segments of the leg are absent in the adult (Mardon et al., 1994). Loss of tissue appears to result from cell death during the larval stage, with resultant failure of leg eversion. In addition, there are three genes with very similar phenotypes that may be involved in such events. Mutations in *fj*, *dachs* or *approximated* all result in loss of growth in portions of the leg and wing in the middle of the PD axis, without affecting the initiation of this axis or the most distal or most proximal differentiation. The molecular identities of these three genes have not previously been described.

fj was described by Waddington (1943), who observed that the tarsus (the most distal portion of the adult leg, composed of five segments) of *fj* adults lacked one of the normal segments and he showed that this loss was already evident in prepupae. The wings were also slightly shortened with the two crossveins closer than normal. He attributed these effects to changes in the relative growth of the parts of the discs. Tokunaga and Gerhart (1976) went on to show that growth was disturbed only in the longitudinal dimension of the leg and by mosaic analysis demonstrated that the gene displayed a local nonautonomy at the joint, most convincingly joint failure in heterozygous tissue that was adjacent to mutant cells. Together, the phenotype and mosaic behavior suggested that *fj* might be a signal regulating growth and patterning along the PD axis.

In the course of an enhancer trap screen for genes affecting regional positional information in the imaginal discs, including the eye and visual system, we isolated an insertion in which the enhancer trap reporter showed a concentric circular pattern of expression in the leg and unusual regional expression in the eye disc and the optic lobes. In this paper, we show that this insertion detects the expression of the *fj* gene. We describe this expression pattern, the recovery of new *fj* alleles, as well as the molecular and biochemical characterization of *fj*. Our results support the hypothesis that fj acts as an intercellular signal involved in regulating growth and differentiation of intermediate portions of the PD axis in both the leg and the wing.

MATERIALS AND METHODS

Fly strains and genetics

Unless otherwise indicated, mutations are as described in Lindsley and Zimm (1992). The wild-type control stock was OregonR. The *fj* enhancer trap line arose in a screen using PlacW (Buckles et al., 1992) and was the kind gift of Robert Rawson and Steven Wasserman (UT Southwestern Medical Center, Dallas, TX).

Histology and immunocytochemistry

Adult legs and wings were dehydrated in alcohol, cleared in xylene and mounted in Permount (Fisher Scientific). Prepupal legs were dissected in phosphate-buffered saline, fixed for 15 minutes in 0.5% glutaraldehyde and mounted in 80% glycerol. Anti-β-galactosidase (β-gal) staining was as described in Ashley and Katz (1994).

Molecular biology

Unless otherwise stated, all standard techniques were as described in Sambrook et al. (1989). An EMBL3 lambda phage genomic library was used for chromosome walking (John Tamkun: UC Santa Cruz, CA). *fj* cDNAs were recovered from a third instar larval eye disc library (Gerald Rubin: UC Berkeley, CA). Double-stranded sequencing of the *fj* cDNA was performed using Sequenase 2.0, or by ABI taq polymerase automated sequencing. The BLASTP sequence comparison program (Altschul et al., 1990) was used to search for homologies.

In situ hybridization

Chromosome in situ hybridization was performed as described in Buckles et al. (1992). For tissue in situ hybridization, the *fj* cDNA subcloned into pBluescript (Stratagene) was used for digoxigenin RNA probe synthesis. Linearized, proteinase K-treated plasmids were used as templates for + and – strand synthesis using the Boehringer Mannheim RNA labeling kit (SP6/T7). Run-off in vitro transcribed RNAs were hydrolyzed in 0.5 N NaOH for 3 hours. Purified, fragmented RNA probes were hybridized overnight to tissues that had been fixed with 4% formaldehyde, proteinase K treated and refixed with 4% formaldehyde and 1% glutaraldehyde. Hybridized tissue was washed and incubated overnight at 4˚C in alkaline phosphatase-conjugated anti-digoxigenin antibody (1:2000) that had been preabsorbed for 60 minutes against dissected, fixed larval carcasses. Enzyme-catalyzed color development used 5-bromo-4-chloro-3-indolyl phosphate and nitroblue tetrazolium salt as substrates. Samples were then dehydrated, cleared in cedarwood oil and xylene, and mounted in Permount.

In vitro translation and translocation assay

For the full-length construct, capped RNA for in vitro translation was synthesized using the Stratagene mRNA synthesis kit. Rabbit reticulocytes and canine pancreatic membranes were purchased from Promega and translation was carried out according to the manufacturer's protocol. The deletion construct was transcribed and translated using Promega's TNT coupled reticulocyte lysate system according to the manufacturer's protocol. The deletion construct was made by digesting the full-length cDNA with the restriction endonuclease Eco0109I (Stratagene), which removed DNA encoding the carboxyterminal 296 amino acids of the ORF. The trypsin protection assay was performed essentially as described (Walter and Blobel, 1983).

For Endoglycosidase H (Endo H) treatment, the translation reaction containing microsomes was overlaid on a cushion of 0.5 M sucrose, 0.025 M KCl and 0.05 M Hepes pH 7.5 and centrifuged for 20 minutes at 100,000 ***g*** in a TL-100 Beckman centrifuge. The microsomal pellet was resuspended in 20 μl of 0.1 M Tris pH 8.0, 1% SDS and 1% β-mercaptoethanol and boiled for 2 minutes. 180 μl of 0.15 M sodium citrate pH 5.5 was added and the reaction was divided into two tubes, 100 μl each. A 1 μl aliquot of 0.1 U of Endo H (Boehringer Mannheim) was added to one tube while the other tube served as a negative control. Reaction was for 6 hours at 37°C. Upon completion, samples were precipitated with trichloroacetic acid and washed with acetone. All samples were boiled with SDS loading buffer for 4 minutes before loading onto a 10% SDS-PAGE gel.

RESULTS

An enhancer trap line with regional expression in the imaginal discs

To identify genes that might play roles in positional specification of the imaginal discs including the eye and visual system, we screened a set of viable enhancer trap lines for regional expression patterns during the third instar larval stage. In the

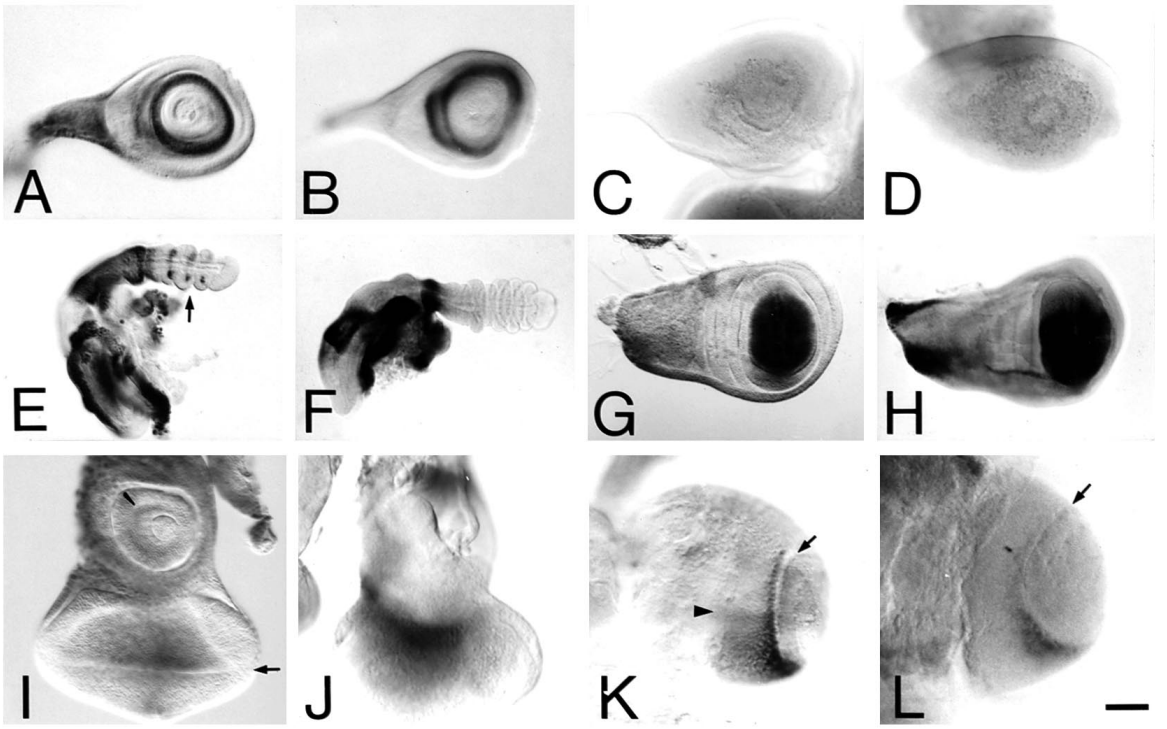

Fig. 1. Expression pattern of *fj*. (A-D) Third instar larval leg disc. (A) Expression pattern of β-gal in the *fj* enhancer trap line visualized with anti-β-gal. The *lacZ* gene is expressed as a fusion with the 5′ portion of the P transposase, which gives the product a nuclear localization. (B-D) Tissue in situ hybridizations (TIS) using an anti-sense *fj* cDNA probe (B) or a positive strand probe (C) against wild-type tissue and an anti-sense probe on fj^2 tissue (D). All remaining panels are displayed as pairs of β-gal staining followed by TIS. Unless noted, all tissue is from third instar larvae. (E,F) 4-6 hour APF prepupal leg discs. The arrow in E points to one of the furrows that mark the prospective tarsal segment boundaries. The difference in staining intensity at these boundaries seen in E and F is likely to be due to perdurance of the β-gal product. (G,H) Wing discs. (I,J) Eye-antennal discs. An arrow marks the morphogenetic furrow and a slash marks one of the antennal arcs of β-gal expression in I. (K,L) Brain lobes. Horizontal view with dorsal at the top and medial to the left. Arrows indicate the furrow that separates the lamina-contributing from the medulla-contributing portions of the ooa. The arrowhead in K points to the position of the dorsal-ventral midline of the underlying medulla neuropil. The scale bar in L represents 23 μm for A-D; 64 μm for E,F; 58 μm for G,H; 25 μm for I,J; and 42 μm for K,L.

enhancer trap method, an engineered P transposable element is inserted randomly into genomic DNA. A *lacZ* gene lacking its own enhancer is carried on the P element and comes under the influence of genomic enhancers near the transposon insertion site (Bellen et al., 1989; Bier et al., 1989; Wilson et al., 1989). The pattern of expression of β-gal has been shown in many cases to predict the expression pattern of nearby endogenous genes. We examined β-gal staining at the late third instar and prepupal stages, a period when axis specification is complete but overt differentiation of each disc has not yet occurred. Based on its provocative expression pattern in the leg disc, eye disc and optic lobes, a single insertion line was chosen for further study.

In the third instar larval leg disc, β-gal was expressed in a pattern of concentric circles (Fig. 1A), similar to a subset of the concentric restrictions that mark the future segment boundaries of the leg. While these patterns tended to overlap in the third instar leg, the localization of this expression was more clearly seen in prepupal leg discs 4-6 hours after puparium formation (APF; Fig. 1E). At this time, eversion of the leg from the folded disc epithelium has just occurred and invaginations marking the future tarsal segment boundaries are clearly visible. A line of positive cells was seen adjacent to each tarsal furrow, with additional strong expression in the first tarsal segment and in the distal tibia. A weaker pattern of semicircular arcs was seen in the antennal discs at the third instar (Fig. 1I). Such expression patterns are predicted for genes involved in setting or reading values along the PD axis of the leg (Bryant, 1993) and suggested this gene might have such a function.

Expression of β-gal in the wing disc was concentrated in the prospective wing blade region, the most distal region of the disc (Fig. 1G).

The β-gal expression patterns in the visual system were unexpected and very unusual. The eye disc is composed of an epithelial sheet interrupted by a moving invagination, the morphogenetic furrow, which progresses from the posterior to the anterior edge of the disc during development. Cells in front of the furrow are unpatterned and actively dividing, while cells immediately posterior to the furrow become recruited into the differentiated clusters that will form the ommatidia of the adult eye (Ready et al., 1976). All genes that have been previously characterized in eye development are expressed uniformly across the width of the eye disc (in parallel to the morphogenetic furrow), reflecting the uniform requirements for photoreceptor and support cell differentiation in each of the repeating units. However, non-uniform expression was observed in *fj* eye discs, with strongest expression in the central

portion of the disc just anterior to the morphogenetic furrow, but with no expression in the lateral regions of the disc (Fig. 1I). An apparent gradient of expression was seen centrally declining toward the posterior tip of the disc. This triangular zone of expression does not correspond to any known developmental or physiological compartment boundaries.

Finally, in the larval brain expression was concentrated in the outer optic anlage (ooa), which forms a circumferential band around the optic lobe (Fig. 1K). The ooa is a proliferation zone that contributes cells to the lamina and distal medulla regions of the optic lobe, which form the postsynaptic targets for the photoreceptor axons. β-gal expression was confined to the ventral portion of this band and only to the part that gives rise to the medulla (see Meinertzhagen and Hanson, 1993, for a discussion of this anatomy). Expression diminished distal to proximal in this zone. A single line of cells continued dorsally along a furrow that separates the lamina from the medulla-contributing portions of the ooa. In a screen of 5000 enhancer trap lines, this was the only gene that we recovered with asymmetric expression in the optic lobes. Such asymmetric distribution suggests a compartment that has not been previously described but which is predicted from work that suggests that the dorsal and ventral halves of the lamina and medulla (which arise from the ooa) are distinguishable by the axons of the photoreceptor neurons (Kunes et al., 1993; Ashley and Katz, 1994).

Staining in the eye and optic lobe were transient and no staining was detectable in adults. However, some β-gal expression persisted in the wings, legs and antennae of adult flies (data not shown).

Generation of mutations and identification of the *fj* gene

Flies containing the original enhancer trap insertion had no detectable phenotype. To create mutations, the P element insertion (PlacW: Bier et al., 1989) was remobilized in the presence of the Δ2-3 transposase (Robertson et al., 1988) and excision lines were identified by loss of the mini-white gene (w^+) carried on the P element. All excision lines were subsequently screened by Southern analysis to confirm that phenotypes occurred only when excision of the P element was accompanied by deletion of adjacent genomic DNA (see below). All such deletion lines were viable; however, they displayed a very specific loss of growth in the middle of the tarsus and in the middle portion of the wing blade (see below).

The insertion site of the P element used to generate these mutations was mapped by chromosome in situ hybridization to the interval 55B,C on chromosome 2R. The previously identified *four-jointed* gene, which maps to the same chromosomal interval as our excision mutations and is uncovered by the same deficiency (Deng and Rizki, 1988), has identical phenotypes in the leg and wing (Lindsley and Zimm, 1992) to those found in our strongest mutations. The single extant allele of *fj* (fj^1) failed to complement our excision mutations, suggesting that these are mutations in the same gene. We therefore named our mutant lines fj^2, fj^3 *and* fj^4, and their phenotypes are described in more detail below.

fj affects growth regionally along the PD axis of the leg and the wing

In the leg, segments occupying intermediate positions in the PD axis were specifically affected in the strongest mutations,

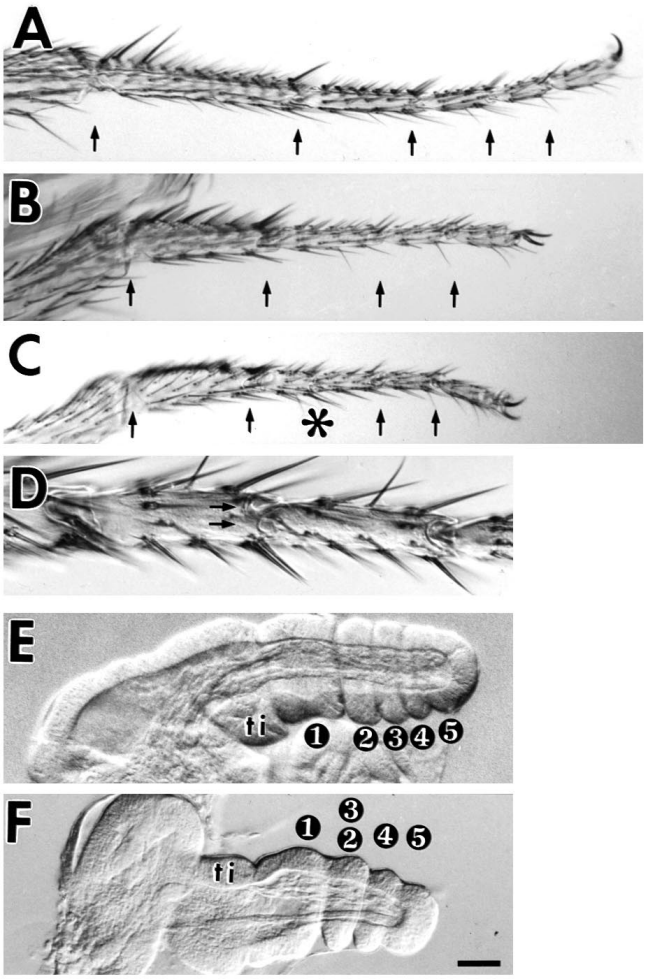

Fig. 2. Leg phenotypes of *fj* excision mutants. Adult female metathoracic legs of wild type (A), fj^2 (B) and fj^4 (C,D). Arrows in A-C mark the positions of the tarsal joints. The asterisk in C marks the position of partial T2/T3 joints, which are shown enlarged in D. (E,F) Prepupal leg discs of wild type (E) and fj^2 (F). The invaginations that mark the future tarsal segment boundaries are already visible and segments 5-1 and the tibia (ti) are indicated. In *fj*, one furrow is already absent and the total length of the leg is reduced. The scale bar in F represents 53 μm for A-C; 30 μm for D; and 26 μm for E,F.

fj^2 and fj^3. The adult leg can be divided into five regions. The most distal portion of the leg is called the tarsus, followed by the tibia, femur, trochanter and coxa more proximally. The tarsus is composed of five segments, T5-T1 (distal to proximal), which are separated from each other by joints and are distinguishable by their lengths, patterns of bristles and cuticular specializations (Fig. 2A). The tarsus was reduced to four segments in these mutants (Fig. 2B). The middle tarsal segments, T2 and T3, were replaced by a single segment that appeared to be a fusion of these two, while T1 (Fig.2B), the tibia and the femur (data not shown) were truncated. The more proximal segments of the leg (the coxa and trochanter) and the most distal (T5 and T4) were unaltered in the mutants. Even within the affected segments, anterioposterior and dorsal-ventral patterning appeared to be normal, based on cuticular patterns.

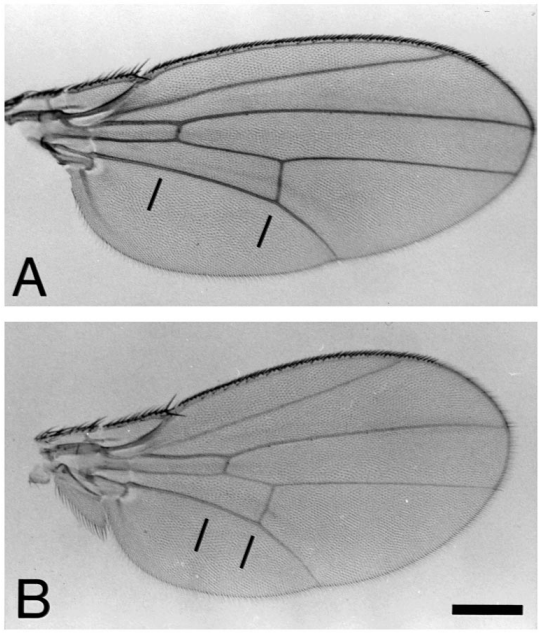

Fig. 3. Adult wing phenotype of *fj*. Wings of wild type (A) and fj^2 (B). The anterior and posterior crossveins are indicated with lines. The intercrossvein distance is significantly reduced in *fj*. The scale bar represents 240 μm.

The size and shape of the adult wing were also altered. These changes were largely the result of a shortened separation between the anterior and the posterior crossveins of the wing (Fig. 3A versus B), an interval that occupies the middle portion of the PD axis in the wing blade. To distinguish between a reduction in cell size versus a reduction in cell number as the origin of this reduced interval, we took advantage of the observation that each cell of the wing blade produces a single hair, consequently the number and density of hairs in any portion of the wing reflects the number of cells (Dobzhansky, 1929). In this manner, the number of cells along the PD axis on a line parallel to vein 4 between the base of the wing blade (at the junction of veins 4 and 5) and the distal wing margin were counted (n=10 wings for each genotype, presented as the average ± s.e.m.). Whereas the cell counts between the vein junction and the anterior crossvein (65.1±1.55, wild type; 68.4±1.61, fj^2) and the posterior crossvein and the wing margin (105±1.52, wild type; 97.5±1.43, fj^2) were similar, the number of cells between the anterior and posterior crossveins in fj^2 were half that of wild type (36.6±0.65, wild type; 16.2±0.83, fj^2). Consequently, we conclude that the reduction in intercrossvein separation seen in the mutant is due to a reduction in total cells in this region, rather than exclusively to a reduced cell size or altered cell shape. As in the leg, dorsal-ventral values appeared to be unaltered in the mutant. There was, however, a slight increase in the separation between the wing veins in the AP dimension (for example, between veins 3 and 4 at their point of widest separation there was an average of 20.7±0.247 cells in wild type versus 24.8±0.420 cells in fj^2). This may be an indirect consequence of the global alteration in wing morphology caused by loss of PD growth. Alternatively, *fj* may have a more subtle but direct effect on growth in the AP axis itself.

The eye was the only other tissue visibly affected in the mutants and the phenotypes observed were mild. In strong *fj* mutants, the external eye showed occasional disordered lens facets and in tangential sections of these eyes a small number of ommatidia (0-33 per eye) appeared to be fused with their neighbors so that they were no longer separated by intervening pigment cells (data not shown). The projections of the photoreceptor neurons to the mutant optic lobes were normal (data not shown).

We also recovered a weaker allele of *fj*, fj^4, which gave phenotypes intermediate between those of the strong alleles and wild-type flies. The legs of fj^4 adults contained either partial joints at the T2/T3 boundary or double partial joints of like polarity at this position (Fig. 2C,D), while a full loss of this joint was rare. Partial joints always occupied the dorsal surface of the leg and showed an incomplete ball and socket invagination, sometimes accompanied by two sensilla campaniformia on the proximal side as in a normal T2/T3 joint. However, the intersegmental membrane on the ventral aspect was absent and the bristle patterns in this area were compressed and distorted slightly on this surface, although bristle pattern elements from each segment were present. This hypomorphic phenotype reinforces the interpretation that *fj* causes a fusion of T2 and T3 rather than loss of either segment. The crossvein separation in the wing was intermediate between that of fj^2 and wild type, while the external eyes appeared to be normal (data not shown).

A deficiency for this region [Df(2R)PC4] uncovered the phenotypes described above with each of our alleles, suggesting these phenotypes result from hypomorphic activity of the gene product. Moreover, the deficiency failed to uncover additional phenotypes so that the restricted loss of PD growth seen in the strong mutants does not appear to result from incomplete loss of gene function (this is supported by the transcript analysis, below, which shows that fj^2 is a null allele).

Loss of PD growth is due to lack of formation rather than degeneration

Loss of growth in the PD axis of the leg and wing might arise from an initial failure in proliferation and differentiation, or might result from a late degeneration event subsequent to proliferation. To distinguish between non-proliferation and degeneration, we observed the emergence of the tarsal segments in prepupal discs that had just begun to evert. By 4 hours APF in wild-type discs, all five of the prospective tarsal segment boundaries can be observed as indentations of the leg epithelium (Fig. 2E). Only four such boundaries were seen in fj^2 discs and the sizes of the presumptive T2/T3 and T1 segments were already abnormally small (Fig. 2F; also see Waddington, 1943). We also looked for, but were unable to detect, any excess cell death by acridine orange staining during the early or late third instar, between the time of active cellular proliferation in the leg disc (Cohen, 1993) and the time of leg eversion that we had monitored (data not shown). These results suggest that the *fj* leg phenotype arises from an initial failure in the proliferation of a subset of tarsal segments, as well as a failure to initiate the T2/T3 segment boundary.

Identification of the *fj* transcript

To learn more about the function of the *fj* gene, we undertook a molecular analysis. Taking advantage of bacterial sequences

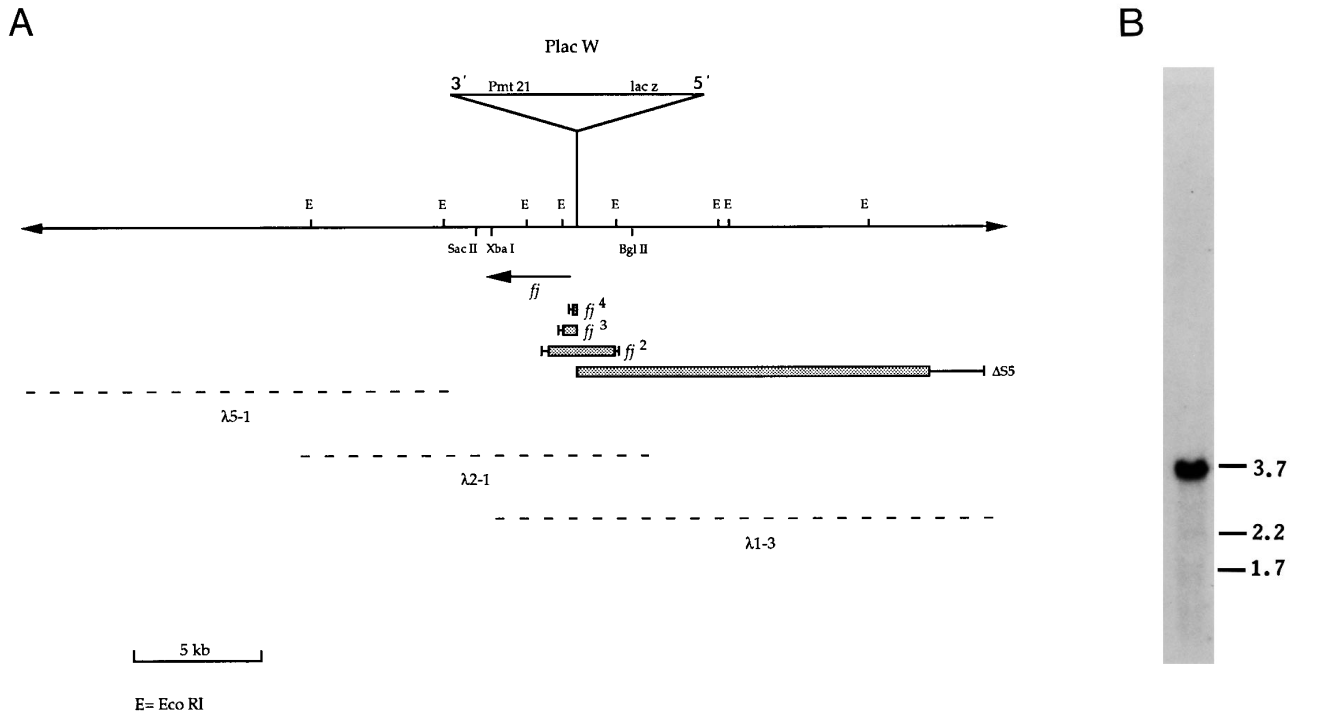

Fig. 4. Map of the *fj* chromosomal region. (A) An *Eco*RI (E) restriction map of the *fj* region is shown. *Sac*II and *Bgl*II (below the line) represent the ends of the two plasmid rescue fragments used to initiate a chromosomal walk in this area. The *Xba*I-*Hin*dIII fragment used to recover the cDNA and for northern analysis extends from the *Xba*I site indicated to a *Hin*dIII site within the P element, approximately 250 bp from its 3′ end. The *fj* transcript, shown under the restriction map (arrow shows direction of transcription, 5′ to 3′), begins 250 bp from the P insertion site. PCR analysis (data not shown) indicates that there are no introns larger than 100 bp in size within this transcript. The extents of the deletions of genomic DNA in four mutant lines are shown below the transcript as hatched boxes. Uncertainties in the breakpoints are marked by bar extensions. fj^2, fj^3 and fj^4 have *fj* phenotypes. The ΔS5 deletion has no detectable phenotype. Lambda genomic clones used to walk across this region are represented by dotted lines. (B) Northern blot of poly(A)$^+$ RNA from wild-type third instar larvae probed with the *Xba*I-*Hin*dIII genomic fragment. A single band of 3.7 kb is observed.

in the PlacW transposon, we recovered flanking genomic fragments by plasmid rescue (Pirrotta, 1986) and used these to isolate genomic phage clones which together contained 40 kb of DNA spanning the transposon insertion site (Fig. 4A). Northern blots across this 40 kb region identified a single 3.7 kb transcript expressed in the third instar/early pupal stages (Fig. 4B), which hybridized to an *Xba*I-*Hin*dIII fragment adjacent to the P element (Fig. 4A; the *Hin*dIII site is located within the 3′ end of the P element). This fragment was then used to isolate cDNAs from a third instar larval cDNA library. A 3.5 kb cDNA was recovered that recognized the 3.7 kb transcript on northern blots (data not shown). Tissue in situ hybridization of wild-type third instar larval tissue (leg, wing, eye and brain) using this cDNA detected roughly the same pattern of expression as the *lacZ* gene in the enhancer trap line (Fig. 1). The only small discrepancy was variable RNA expression at the segment boundaries in the prepupal tarsus (Fig. 1E,F; see Discussion). We conclude that the enhancer trap is detecting the expression pattern of the 3.7 kb transcript.

All of the w^+ revertants with a *fj* phenotype had deletions within the 3.7 kb transcript. The extent of the deletions in fj^2, fj^3 and fj^4 are shown in Fig. 4A. The strongest mutations, fj^2 and fj^3, interrupt this transcript. Indeed, no transcript is detectable in fj^2 by in situ hybridization when the cDNA is used as a probe (Fig. 1D), confirming that this is a null allele. fj^4 eliminates sequences at the 5′ end of the transcript and most likely affects the regulation rather than the integrity of the gene product, resulting in a weaker phenotype than the null mutations.

Structure of the *fj* gene product

We believe the 3.5 kb cDNA corresponds to the *fj* gene based on both its pattern of expression and the correspondence between *fj* mutations and interruptions of the transcript this cDNA represents. We therefore proceeded to sequence this cDNA.

The 3.5 kb cDNA contains an open reading frame (ORF) that encodes a polypeptide of 583 amino acids, with a predicted molecular weight of 65,504 and a pI of 8.70 (Fig. 5). The AUG at position 1 of the ORF is consistent with the consensus translation initiation site for *Drosophila* (Cavener and Ray, 1991) and is preceded by stop codons in all three frames. The next methionine, at position 62, does not match this consensus. Although the predicted ORF has no similarity to any known gene in the available data bases, several structural motifs are present. The Kyte-Doolittle Hydropathy test (Kyte and Doolittle, 1982) detects a potential membrane spanning region at amino acids 77-101 but no comparable region at the N terminus that would correspond to a signal sequence (Fig. 5). The charge distribution surrounding this potential transmembrane region strongly predicts (Hartmann et al., 1989) that the polypeptide should be oriented with its N terminus inside the

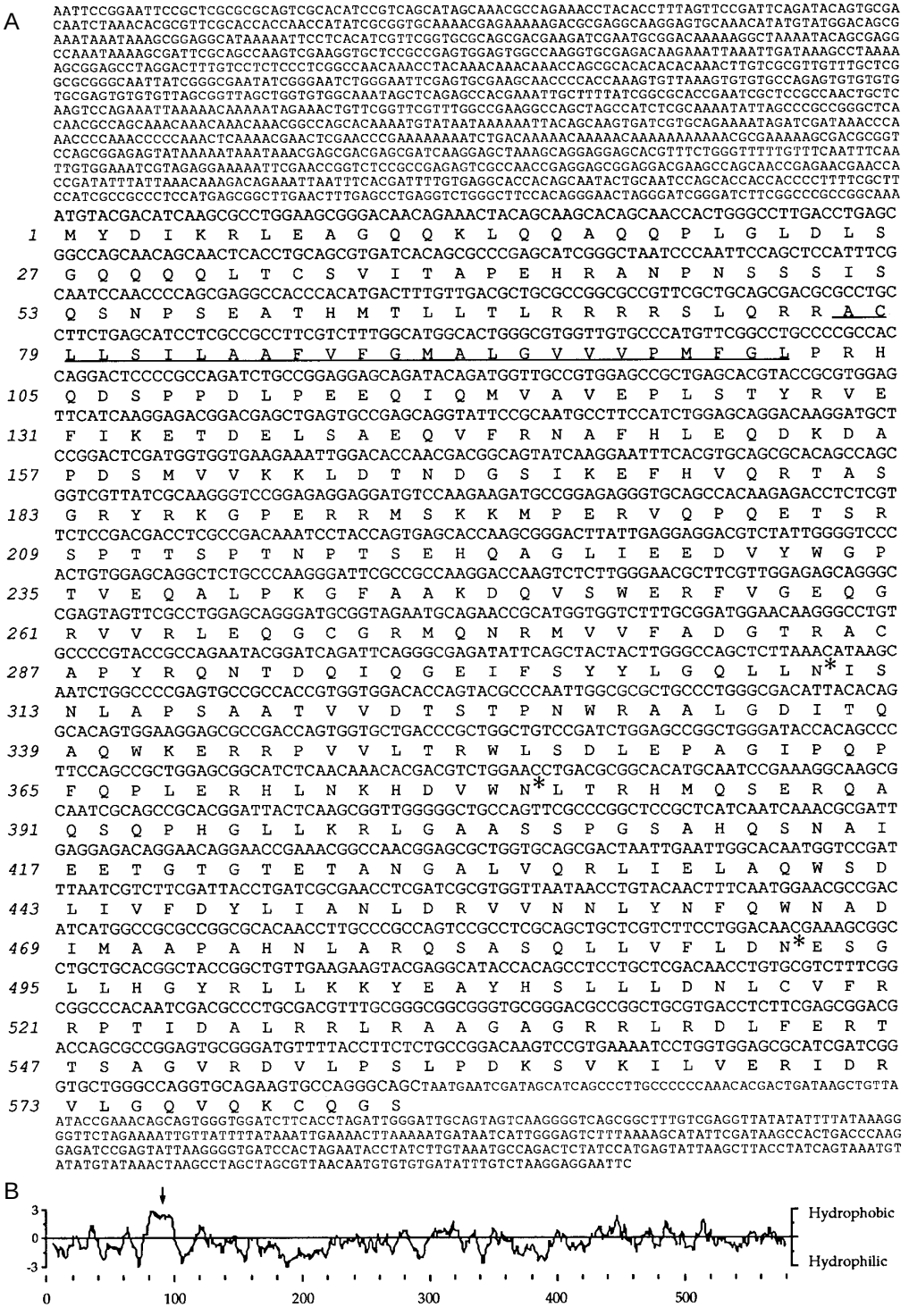

Fig. 5. Sequence of the *fj* cDNA. (A) The nucleotide sequence and amino acid conceptual translation of the *fj* cDNA. The maximum potential transmembrane region of 26 amino acids is underlined. The von Heijne algorithm predicts a potential signal sequence cleavage site between residues 89 and 90 (score = 7.25; cutoff for significance is 6.0) and 93 and 94 (score = 6.06). Although these are in the middle of the hydrophobic region, slippage of the membrane spanning residues could expose the latter pair at the end of the membrane pore and thus make it accessible to signal peptidase. Potential glycosylation sites in the C-terminal domain, which appears to be extracellular, are indicated with asterisks. A PEST sequence is found between amino acid residues 209 and 220, and an alpha-amidation consensus sequence (X-G-R-R) at residues 535-538. There are 14 pairs of basic residues, 10 in the C-terminal domain. This sequence has been submitted to the NCBI GenBank data base (accession no. U28837). (B) Kyte-Doolittle Hydropathy plot. A hydrophobic cluster consistent with a transmembrane region is found between residues 77 and 101, and is indicated with an arrow.

cell and its C-terminal domain external, as in a type II membrane protein. Two sites within the hydrophobic region give a significant score in the von Heijne algorithm (von Heijne, 1986), which predicts cleaved signal sequences. Although the algorithm was modeled on N-terminal signal sequences and has not been tested extensively with internal signal sequences of type II membrane proteins, it was successful in predicting a cleavage site in the *Drosophila hedgehog* (*hh*) protein, which has a similar structure to *fj* (Lee et al., 1992; Tabata and Kornberg, 1994). Cleavage at either of the predicted sites in the fj protein would allow the mature C-terminal polypeptide chain to be released into the lumen of the rough endoplasmic reticulum and eventually secreted. The sequence also contains 14 pairs of adjacent basic residues, which may serve as sites for post-translational proteolytic processing; a consensus site for alpha-amidation near the C terminus (a common modification in proteolytically processed neuropeptides: Eipper et al., 1992); and a PEST sequence

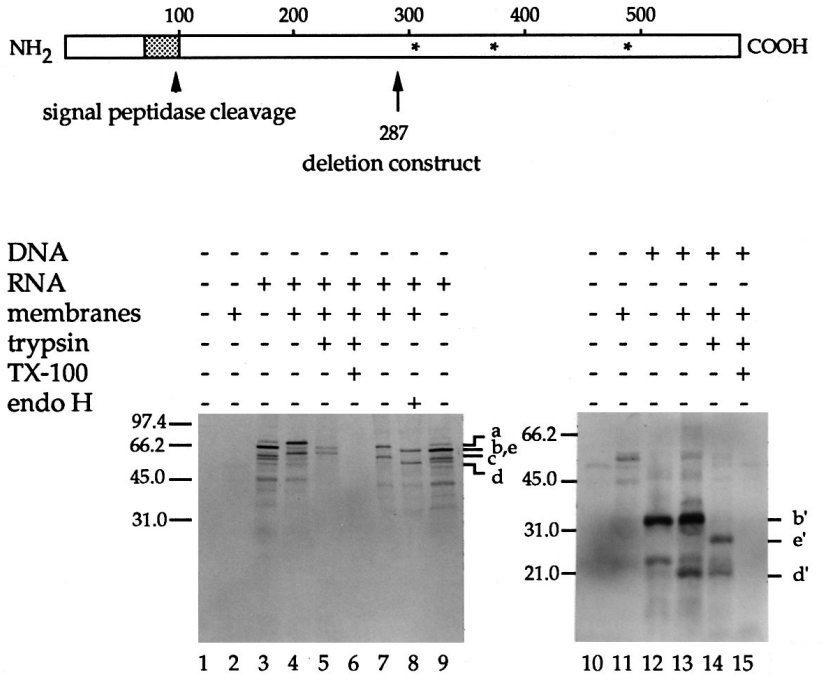

Fig. 6. In vitro analysis of fj biosynthesis. The diagram at top shows the full-length fj protein. The shaded box represents the transmembrane domain and asterisks denote the locations of predicted asparagine-linked glycosylation sites in the C-terminal portion of the molecule. An arrowhead shows the approximate site of signal peptidase cleavage. A truncated protein containing the first 287 amino acids of fj (indicated by an arrow) was generated by cleavage of the full-length cDNA. The truncated cDNA was analyzed directly in a coupled transcription-translation reaction. fj mRNA (lanes 1-9, full length; lanes 10-15, truncated) was translated in a reticulocyte lysate in the presence or absence of canine pancreatic microsomal membranes and with additions as indicated. 10% SDS-PAGE gels are shown. Bands a-e and b′, d′ and e′ are referred to in the text. The migration of molecular weight markers is indicated to the left of each gel.

(Rogers et al., 1986). Finally, there are four consensus sites for asparagine-linked glycosylation, three in the C-terminal domain.

In vitro analysis of fj biosynthesis

To test the predicted size, topology, glycosylation and potential cleavage of the fj protein, an in vitro transcription-translation-coupled translocation assay was performed using rabbit reticulocytes and canine pancreatic microsomes (Fig. 6). To minimize ambiguity, both full-length (lanes 1-9) and truncated (lanes 10-15) cDNAs were transcribed, translated and analyzed on SDS-polyacrylamide gels. Truncation at amino acid 287 (Fig. 6, top) eliminates the potential glycosylation sites in the C-terminal domain and moves the migration of the resultant proteins to a size range where small molecular weight differences are exaggerated in the gel system that we employed. Both of these features simplify the interpretation of the pattern of proteins produced by translation and processing, and we will therefore discuss this construct first.

When the truncated cDNA was analyzed in this system, a major band of 33×10^3 M_r (b′ in Fig. 6) was produced in both the absence (lane 12) and presence (lane 13) of membranes but not in the absence of fj DNA (lanes 10 and 11). This corresponds to the unglycosylated protein expected from translation of the truncated mRNA. A second minor band of 24×10^3 M_r was also produced, which may represent initiation at the second methionine (amino acid 62). When the membranes were challenged with trypsin (lane 14) a 28×10^3 M_r polypeptide (e') was protected, as expected if the larger C-terminal domain of the 33×10^3 M_r species had been translocated into the lumen of the microsomes and the protein were then cleaved by trypsin just N-terminal to the membrane. The size of the protected fragment is inconsistent with translocation of the N-terminal polypeptide, which is much smaller. fj must therefore be synthesized as a type II membrane protein. In the presence of membranes, a new band of 22×10^3 M_r (d′) was also produced that was subsequently protected from trypsin digestion. This polypeptide is the size predicted for the signal peptidase-cleaved C-terminal domain of the truncated protein, which would be wholly sequestered by the membranes.

The interpretation of the full-length protein is more complicated, but the data are consistent with these observations. A major band of 67×10^3 M_r (b) was observed when full-length *fj* mRNA was translated in the absence of microsomes (lanes 3 and 9), consistent with the predicted ORF. Several faster migrating species of a lower intensity were also frequently seen. The origin of these bands is unclear. Two new bands (a,c) appeared when RNA was translated in the presence of membranes (lanes 4 and 7). The migration of both of these bands increased after treatment with Endo H (lane 8), which cleaves asparagine-linked high mannose glycans added cotranslationally in the microsomes. This confirms that fj is inserted into membranes and glycosylated. The larger deglycosylated membrane protein comigrates with the major polypeptide produced in the absence of microsomes and therefore is likely to correspond to the full-length protein. The lower band in the Endo H lane (d) migrates at a position approximately 10×10^3 M_r smaller than the full-length protein and does not comigrate with any of the minor bands produced in the absence of microsomes. The migration of this band is consistent, however, with that expected for the signal peptidase-cleaved C-terminal domain predicted by the von Heijne algorithm.

Potential asparagine-linked glycosylation sites exist in both the N- and C-terminal regions of the sequence. If the N-terminal glycosylation site was utilized, we would expect an alteration in the migration of the truncated construct in the presence of microsomes, but no alteration was observed. To confirm that the C-terminal peptide (482 amino acids) and not the N-terminal peptide (76 amino acids) was translocated into the lumen of the microsomal vesicles, microsomes were treated with trypsin in the presence (lane 6) and absence (lane 5) of

detergent. All protein was susceptible to protease in the presence of detergent. In its absence, the membranes protected two fragments of 67×10^3 M_r (e) and 63.5×10^3 M_r (c). Both bands are within the size range expected for the C-terminal peptide, consistent with the proposed type II topology and inconsistent with a type I membrane glycoprotein. Cleavage of the full-length protein at lysine and arginine residues N-terminal to the transmembrane region would account for the generation of the 67×10^3 M_r polypeptide. The 63.5×10^3 M_r polypeptide comigrates with the putative signal peptidase-cleaved C-terminal domain. Such a secreted polypeptide would be wholly sequestered by the membrane and therefore unavailable to further proteolytic digestion, as observed.

Together, these results indicate that *fj* encodes a type II membrane glycoprotein and strongly suggest that, at least in this in vitro system, fj is synthesized in both a membrane-bound and a secreted form.

DISCUSSION

Previous work on the *fj* gene suggested that it functions as a regional signalling molecule regulating growth and differentiation in specific portions of the PD axis in the leg and wing. Our analysis of the phenotype, expression pattern, molecular identity and biochemistry of fj strongly supports this hypothesis.

A role in intercellular communication may be inferred from the nonautonomous behavior of wild-type cells juxtaposed with mutant cells in mosaic patches at the T2/T3 boundary in the leg (Tokunaga and Gerhart, 1976). The heterozygous cells immediately adjacent to the mutant patch failed to form a joint. This would be expected if a defective signal from the mutant cells was unable to stimulate a receptor on the immediately adjacent wild-type cells. However, the majority of *fj* clones crossing the T2/T3 segment boundary displayed autonomous failure to form a joint (the nonautonomous group were attributed to probable mitotic recombination between the marker and the *fj* gene), suggesting *fj* may be required in both cells. A nonautonomous signal or ligand would presumably be in the form of a cell surface or secreted molecule, although the molecule defective in the mosaics could also be involved in the generation of the signal. Our analysis of the *fj* gene product is consistent with the fj protein representing the signal itself.

Conceptual translation of *fj* cDNA predicts a type II transmembrane glycoprotein with a potential internal signal peptidase cleavage site. In vitro translation of *fj* mRNA in the presence of membranes results in cleavage of a portion of the nascent polypeptides at the predicted site. However, the microsomal cleavage of fj is incomplete and a significant portion of the protein remains transmembrane and full length. This was also observed in in vitro experiments with the hh protein (Lee et al., 1992), the only other *Drosophila* type II membrane protein known in which the transmembrane region functions as a cleavable signal sequence. hh was subsequently shown to be more completely processed in vivo (Tabata and Kornberg, 1994). Incomplete cleavage in vitro may be due to inefficient processing by the heterologous microsomal membranes used in these experiments. Alternatively, it may be a normal property of fj with the secreted and transmembrane forms serving potentially different functions (for precedents with other growth factors see: Massague and Pandiella, 1993). Regulated proteolysis could then control the relative abundance of each form. If fj is indeed secreted, the ten dibasic residues found in the C-terminal domain of the fj protein may be sites for further proteolytic processing and regulation.

We believe that *fj* is required for local proliferation in imaginal tissue. Firstly, loss of function results in a loss of tissue in both the leg and the wing. In the leg, a loss of growth is apparent as early as the prepupa and we have been unable to identify any abnormal cell death between the time of cell proliferation cessation and this period that could otherwise account for this absence. Secondly, *fj* is strongly expressed in known proliferation zones including the region of proliferation just anterior to the morphogenetic furrow of the eye disc and the outer proliferation center of the optic lobe. Although we have seen only mild phenotypes in the eye, Waddington (1943) observed that the eye is greatly diminished or lost in double mutants of *fj* and *dachsous (ds)*, a gene with homology to cadherins (Hortsch and Goodman, 1991) that by itself has no phenotype in the eye. A role for *fj* in controlling growth of the eye may therefore be masked by the activity of other genes. Thirdly, two distinct tumor-suppressor genes, *Gull* (Bryant et al., 1988; Mahoney et al., 1991) and *expanded* (Boedigheimer and Laughon, 1993), are able to suppress the *fj* leg phenotype in double mutants (Villano and Katz, unpublished observations) suggesting that loss of fj can be compensated for by deregulation of proliferative activity. Whether fj is sufficient for growth can be tested by ectopic expression. However, if fj is indeed a signal then the effect of ectopic expression will depend on the distribution of its receptor and downstream intracellular signalling pathways, which may not be ubiquitous. Moreover, growth is broadly defined and may involve the activation of transcriptional programs, cell-cycle regulation, or regulation of cell-cell contacts that themselves serve as mitogenic and differentiation signals.

The expression pattern of *fj* RNA, visualized by both in situ hybridization and β-gal expression in the enhancer trap allele, is also consistent with fj serving as a localized, regional signal and is congruous with the phenotypes observed. In the prepupal leg, fj is expressed in a circumferential ring adjacent to each tarsal segment boundary, including the T2/T3 segment boundary that is lost in the mutant, and within T1 and the distal tibia, which are both truncated. Its association with invaginations in the leg suggest these may be important signalling centers for proliferation, similar to the furrows of the eye and optic anlage with which *fj* is also associated. However, *fj* is also expressed at segment boundaries that are unaffected in the null mutant, specifically T5/T4 and T4/T3 and in the antennal disc, where we have never seen a phenotype. Similarly, while *fj* expression is limited to the prospective wing blade area of the wing disc, the area of expression is broader than that predicted by the loss-of-function phenotype. Finally, despite strong expression in the eye disc and optic lobe, we see only subtle phenotypes in these tissues. One possibility is that the receptor or partner used by this protein is even more tightly restricted than fj itself (as, for example, in the *sevenless-bride of sevenless* interaction: Van Vactor et al., 1991). Alternatively, fj activity may be concealed by the redundant activities of other genes at these positions, as appears to be the case in the eye disc (above and our unpublished observations).

Several slight discrepancies were observed between the β-gal pattern of the enhancer trap and the in situ hybridization analysis, most notably the variable or absent expression of

RNA at the distal tarsal boundaries in the prepupal leg. We believe the expression in the enhancer trap represents a perdurance of the β-gal protein past the time that *fj* RNA is normally turned off. This perdurance allows us to infer that fj is transiently expressed at the forming segment boundaries of the tarsus during their period of proliferation and growth and is turned off at the beginning of the elongation and evagination phase of disc morphogenesis. Similarly, the anterior-posterior gradient of β-gal expression between the morphogenetic furrow and the optic stalk in the eye disc may represent the perdurance of β-gal left behind as the morphogenetic furrow moved and broadened from posterior to anterior, with strongest RNA expression just in front of the furrow. A similar conclusion may apply to the much stronger medial-lateral gradient in the ooa observed with β-gal in the enhancer trap allele.

In summary, the diverse segments of a limb are thought to be formed through the readout of differential information along a proximal-distal axis, yet very little is known about how such an axis might be interpreted. *fj* and similar genes are likely to provide important clues to these events. Recent work has shown that molecules used in initiating the PD axis in flies are also used to initiate the limb bud in vertebrates (see Smith, 1994 for a review), demonstrating a remarkable conservation in genes and strategies. It will be of some interest to learn if the molecular strategies used to interpret this axis and to control growth regionally along the limb are similarly conserved.

We would like to thank the following individuals and centers for fly stocks: Eric Wieschaus, and the Indiana and Bowling Green Stock Centers. We would also like to thank Robert Rawson for bringing the fj enhancer trap line to our attention, Gerald Rubin for the third instar larval eye disc library, John Tamkun for the EMBL3 genomic library, Jackie Nguyen for help with the excision screen, Gerri Buckles for technical assistance, Carl Sidle for his excellent photographic work, Scott Rose for help with sequencing, Ngoc Nguyen for helpful discussions and members of the laboratory for their suggestions and assistance throughout this project. We especially acknowledge the expert technical assistance of Jennifer Ashley. We are grateful to Leon Avery, Dennis McKearin and Steven Wasserman for extremely helpful comments on the manuscript. This work was supported by the Council for Tobacco Research, USA (to F. N. K.) and a Perot Family Foundation Scholarship (to J. L. V.).

REFERENCES

Agnel, M., Roder L., Griffin-Shea, R. and Vola, C. (1992). The spatial expression of *Drosophila rotund* gene reveals that the imaginal discs are organized in domains along the proximal-distal axis. *Roux's Arch. Dev. Biol.* **201**, 284-295.

Altschul, S. F., Gish W., Miller, W., Myers, E. W. and Lipman, D. J. (1990). Basic local alignment search tool. *J. Mol. Biol.* 215, 403-410.

Ashley, J. A. and Katz, F. N. (1994). Competition and position-dependent targeting in the development of the *Drosophila* R7 visual projections. *Development* **120**, 1537-1547.

Basler, K. and Struhl, G. (1994). Compartment boundaries and the control of *Drosophila* limb pattern by *hedgehog* protein. *Nature* **368**, 208-214.

Bellen, H. J., O'Kane, C.J., Wilson, C., Grossniklaus, U., Pearson, R.K. and Gehring, W. J. (1989). P-element-mediated enhancer detection: a versatile method to study development in *Drosophila*. *Genes Dev.* **3**, 1288-1300.

Bier, E., Vaessin, H., Shepherd, S., Lee, K., McCall, K., Barbel, S., Ackerman, L., Carretto, R., Uemura, T., Grell, E., Jan, L. Y. and Jan, Y. N. (1989). Searching for pattern and mutation in the *Drosophila* genome with a P-lacZ vector. *Genes Dev.* **3**, 1273-1287.

Boedigheimer, M. and Laughon, A. (1993). *expanded*: a gene involved in the control of cell proliferation in imaginal discs. *Development* **118**, 1291-1301.

Bryant, P. J. (1993). The polar coordinate model goes molecular. *Science* **259**, 471-472.

Bryant, P. J., Huettner, B., Held, L. I., Ryerse, J. and Szidonya, J. (1988). Mutations at the *fat* locus interfere with cell proliferation control and epithelial morphogenesis in *Drosophila*. *Dev. Biol.* **129**, 541-554.

Buckles, G. R., Smith, Z. D. M. and Katz, F. N. (1992). *mip* causes hyperinnervation of a retinotopic map in *Drosophila* by excessive recruitment of R7 photoreceptor cells. *Neuron* **8**, 1015-1029.

Campbell, G., Weaver, T. and Tomlinson, A. (1993). Axis specification in the developing *Drosophila* appendage: the role of *wingless, decapentaplegic*, and the homeobox gene *aristaless*. *Cell* **74**, 113-1123.

Cavener, D. R. and Ray, S. C. (1991). Eukaryotic start and stop translation sites. *Nucleic Acids Res.* **19**, 3185-3192.

Chasan, R. and Anderson, K. V. (1993). Maternal control of dorsal-ventral polarity and pattern in the embryo. In *The Development of Drosophila melanogaster* (ed. M. Bate and A. Martinez Arias), Vol. I. pp 387-424. Cold Spring Harbor, NY: Cold Spring Harbor Laboratory Press.

Cohen, S. M. (1993). Imaginal disc development. In *The Development of Drosophila melanogaster* (ed. M. Bate and A. Martinez Arias), Vol.II. pp 747-841. Cold Spring Harbor, NY: Cold Spring Harbor Laboratory Press.

Cohen, S. M., Bronner, G., Kuttner, F., Jurgens, G. and Jackle, H. (1989). *Distal-less* encodes a homoeodomain protein required for limb development in *Drosophila*. *Nature* **338**, 432-434.

Couso, J. P., Bate, M. and Martinez-Arias, A. (1993). A *wingless*-dependent polar coordinate system in *Drosophila* imaginal discs. *Science* **259**, 484-489.

Deng, Y. and Rizki, T. M. (1988). Genetic and developmental analysis of the A1 phenoloxidase of *Drosophila*. *Genome* **30 (Suppl. 1)**, 192.

Diaz-Benjumea, F. J., Cohen, B. and Cohen, S. M. (1994). Cell interaction between compartments establishes the proximal-distal axis of *Drosophila* legs. *Nature* **372**, 175-179.

Dobzhansky, T. (1929). The influence of the quantity of chromosomal material on the size of the cells in *Drosophila melanogaster*. *Wilhelm Roux's Arch. EntwMech. Org.* **115**, 363-379.

Driever, W. (1993). Maternal control of anterior development in the *Drosophila* embryo. In *The Development of Drosophila melanogaster* (ed. M. Bate and A. Martinez Arias), vol. I. pp 301-323. Cold Spring Harbor, NY: Cold Spring Harbor Laboratory Press.

Eipper, B. A., Stoffers, D. A. and Mains, R. E. (1992). The biosynthesis of neuropeptides: peptide α-amidation. *Annu. Rev. Neurosci.* **15**, 57-85.

Fristrom, D. and Fristrom, J. W. (1993). The metamorphic development of the adult epidermis. In *The Development of Drosophila melanogaster* (ed. M. Bate and A. Martinez Arias), vol.II. pp 843-897. Cold Spring Harbor, NY: Cold Spring Harbor Laboratory Press.

Godt, D., Couderc, J. L., Cramton, S. E. and Laski, F. A. (1993). Pattern formation in the limbs of *Drosophila*: *bric a brac* is expressed in both a gradient and a wave-like pattern and is required for specification and proper segmentation of the tarsus. *Development* **119**, 799-812.

Hartmann, E., Rapoport, T. A. and Lodish, H. F. (1989). Predicting the orientation of eukaryotic membrane-spanning proteins. *Proc. Natl. Acad. Sci. USA* **86**, 5786-5790.

Hortsch, M. and Goodman, C. S. (1991). Cell and substrate adhesion molecules in *Drosophila*. *Ann. Rev. Cell Biol.* **7**, 505-557.

Kerridge, S. and Thomas-Cavallin, M. (1988). Appendage morphogenesis in *Drosophila*: a developmental study of the rotund (*rn*) gene. *Roux's Arch Dev Biol.* **197**, 19-26.

Kunes, S., Wilson, C. and Steller, H. (1993). Independent guidance of retinal axons in the visual system of *Drosophila*. *J. Neurosci.* **13**, 752-767.

Kyte, J. and Doolittle, R. F. (1982). A simple method for displaying the hydropathic character of a protein. *J. Mol. Biol.* **157**, 133-148.

Lee, J. J., von Kessler, D. P., Parks, S. and Beachy, P. A. (1992). Secretion and localized transcription suggest a role in positional signaling for products of the segmentation gene *hedgehog*. *Cell* **71**, 33-50.

Lindsley, D. L. and Zimm, G. G. (1992). *The Genome of Drosophila melanogaster*. New York.

Mahoney, P. A., Weber, U., Onofrechuk, P., Biessmann, H., Bryant, P.J. and Goodman, C. S. (1991). The *fat* tumor suppressor gene in *Drosophila* encodes a novel member of the cadherin gene superfamily. *Cell* **67**, 853-868.

Mardon, G., Solomon, N. M. and Rubin, G. M. (1994). *dachshund* encodes a nuclear protein required for normal eye and leg development in *Drosophila*. *Development* **120**, 3473-3486.

Massague, J. and Pandiella, A. (1993). Membrane-anchored growth factors. *Annu. Rev. Biochem.* **62**, 515-541.

Meinertzhagen, I. A. and Hanson, T. E. (1993). The development of the optic lobe. In *The Development of Drosophila melanogaster* (ed. M. Bate and A. Martinez Arias), vol. II. pp 1363-1491. Cold Spring Harbor, NY: Cold Spring Harbor Laboratory Press.

Pirrotta, V. (1986). Cloning *Drosophila* genes. In *Drosophila, A Practical Approach* (ed. D.B. Roberts), pp 83-110. Oxford: IRL Press.

Ready, D. F., Hansen, T. J. E. and Benzer, S. (1976). Development of the *Drosophila* retina, a neurocrystalline lattice. *Dev. Biol*. **53**, 217-240.

Robertson, H. M., Preston, C. R., Phillis, R. W., Johnson-Schlitz, D. M., Benz, W. K. and Engels, W. R. (1988). A stable genomic source of P element transposase in *Drosophila melanogaster*. *Genetics* **118**, 461-470.

Rogers, S., Wells, R. and Rechsteiner, M. (1986). Amino acid sequences common to rapidly degraded proteins: the PEST hypothesis. *Science* **234**, 364-368.

Sambrook, J., Fritsch, E. F. and Maniatis, T. (1989). *Molecular Cloning, A Laboratory Manual*. Cold Spring Harbor, NY: Cold Spring Harbor Laboratory Press.

Schneitz, K., Spielmann, P. and Noll, M. (1993). Molecular genetics of *aristaless*, a prd-type homeo box gene involved in the morphogenesis of proximal and distal pattern elements in a subset of appendages in *Drosophila*. *Genes Dev.* **7**, 114-129.

Smith, J. C. (1994). Hedgehog, the floor plate, and the zone of polarizing activity. *Cell* **76**, 193-196.

Sprenger, F. and Nusslein-Volhard, C. (1993). The terminal system of axis determination in the *Drosophila* embryo. In *The Development of Drosophila melanogaster* (ed. M. Bate and A. Martinez Arias), vol. I. pp 365-386. Cold Spring Harbor, NY: Cold Spring Harbor Laboratory Press.

St. Johnston, D. (1993). Pole plasm and the posterior group genes. In *The Development of Drosophila melanogaster* (ed. M. Bate and A. Martinez Arias), vol. I. pp 325-364. Cold Spring Harbor, NY: Cold Spring Harbor Laboratory Press.

Tabata, T. and Kornberg, T. B. (1994). *Hedgehog* is a signaling protein with a key role in patterning *Drosophila* imaginal discs. *Cell* **76**, 89-102.

Tokunaga, C. and Gerhart, J. C. (1976). The effect of growth and joint formation on bristle pattern in *D. melanogaster*. *J. Exp. Zool*. **198**, 79-96.

Van Vactor, Jr. D. L., Cagan, R. L., Kramer, H. and Zipursky, S. L. (1991). Induction in the developing compound eye of *Drosophila*: multiple mechanisms restrict R7 induction to a single retinal precursor cell. *Cell* **67**, 1145-1155.

von Heijne, G. (1986). A new method for predicting signal sequence cleavage sites. *Nucleic Acids Res.* **14**, 4683-4690.

Waddington, C. H. (1943). The development of some ‘leg genes’ in *Drosophila*. *J. Genet*. **45**, 29-43.

Walter, P. and Blobel, G. (1983). Preparation of microsomal membranes for cotranslational protein translocation. *Meth. Enzymol*. **96**, 682-691.

Wilson, C., Pearson, R. K., Bellen, H. J., O’Kane, C. J., Grossniklaus, U. and Gehring, W. J. (1989). P-element-mediated enhancer detection: an efficient method for isolating and characterizing developmentally regulated genes in *Drosophila*. *Genes Dev*. **3**, 1301-1313.

(Accepted 15 June 1995)